

Wistar and Sprague-Dawley rats demonstrate distinct features of metabolic profile after acute myocardial infarction

Yue Zheng

Tianjin Medical University

Qiang Zhang

Tianjin Third Central Hospital

Wenxuan Xu

Tianjin Medical University

Zhihuan Dong

Tianjin Medical University

Lei Huang

Tianjin Third Central Hospital

Lei Zhang

Tianjin Third Central Hospital

Tong Li (✉ litong3zx@sina.com)

Tianjin Third Central Hospital <https://orcid.org/0000-0002-6281-5163>

Research article

Keywords: metabolic profile, myocardial infarction, clinical research, rat, metabolic pathway

Posted Date: August 9th, 2019

DOI: <https://doi.org/10.21203/rs.2.12566/v1>

License: © ⓘ This work is licensed under a Creative Commons Attribution 4.0 International License. [Read Full License](#)

Abstract

Background: Wistar and Sprague-Dawley (SD) Outbred Rat can be considered the standard rodents for acute myocardial infarction (AMI). However, a direct comparison between Wistar and SD Rat as models of AMI has not been adequately evaluated so far. **Methods:** MI was constructed and cardiac functions were measured to show the success of model construction. The metabolites among Wistar, SD rats and patients with AMI were screened, respectively, and further three groups and subgroups metabolic pathway analysis was applied through MetaboAnalyst 4.0. **Results:** The animal MI model was constructed successfully. All the QC samples we inserted qualified, which allowed us to confirm that the analytical results were valid. After screening by three methods, there are 42 significant plasma metabolites determined in our study, which consist of 19, 18 and 23 metabolites in Wistar, SD rats and human with AMI, respectively. Therefore, to discuss the similarity of Wistar and SD rats to human, SD rats and human had two similar screened metabolic pathways, whereas Wistar rats and human had three screened metabolic pathways. Through subgroup analysis, Glycerophospholipid metabolism was only one which possessed metabolic pathway difference and did not affected by age and time, whereas Sphingolipid metabolism increased only in AMI when compared to SHAM group. **Conclusions:** Sphingolipid metabolism in SD rats is not suggested to be substitute for human metabolic research and the effect of Wistar rats on metabonomic is better than that of SD rats because their metabolic pathways are relatively closer to human's real world.

Background

Cardiovascular diseases are associated with considerable mortality and morbidity(1). Acute myocardial infarction (MI) is caused mostly by the interruption and a sharp reduction of coronary ischemia. As a result, myocardial necrosis happens because of an acute ischemia hypoxia severely and enduringly(2). There is a high risk of death in the acute phase of myocardial infarction and the chronic phase is featured with ventricular remodeling and heart failure. The clinical manifestations of ventricular remodeling are the expansion of left ventricular, thinning of wall-thickness, decrease in the systolic and diastolic functions(3). It is a pathological process which is closely related with hemodynamic disorder and if it goes for a long time, chronic heart failure will come into being involving a variety of biological signals' pathway regulation(4).

For a better understanding of these pathologies and to evaluate potential treatments for the metabolic syndrome, a number of experimental animal models have been developed(5). Despite the multifactorial etiology of MI, the increasing morbidity suggests that environmental and behavioral factors seem to be the major contributors to the MI incidence rather than genetic changes. However, genes and pathways should still be investigated.

Wistar and Sprague-Dawley (SD) Outbred Rat can be considered the standard rodents for this experiment type. Furthermore, due to their larger size, the evaluation of some metabolic parameters such as blood pressure is facilitated over mice. However, they are susceptible to diet-induced obesity and insulin resistance with individual variations(6). What is worse, we have not known the homology between operation-induced MI and spontaneous MI, for example, human's atherosclerosis- or high-lipid-related MI. So, the first thing we should know is to investigate the difference of metabolic profile between Wistar and SD Rat in usual status after MI.

However, a direct comparison between Wistar and SD Rat as models of MI has not been adequately evaluated so far. There are studies reporting some metabolic changes caused by special diet in Wistar but not in SD rats(7, 8). Nevertheless, it is difficult to attribute those variations to the strain of the animal used since there are other variables like the age of animals, the duration of the study and the composition of the diet used that can also be behind those divergences.

In the present study, Wistar and SD rats were studied in parallel to evaluate the metabolic effects of MI groups in comparison to SHAM groups, in both strains. To assess some of the features of the metabolic syndrome, functional evaluations were performed, for example, electrocardiogram (ECG), cardiac output (CO) and heart rate (HR). Given the growing body of evidence demonstrating the prominent role of metabolic profile, the metabonomic after MI were also evaluated in both strains. Therefore, the present study aimed to evaluate whether the metabolic profiles of Wistar and SD rats expressed after MI are the same as the samples of human being and may serve as targets for further LV remodeling researches. Additionally, we determined the metabolic profile of human samples to compare with those of Wistar and SD rats after MI.

Methods

2.1 Animals

Wistar rats and Sprague-Dawley (SD) male rats (SPF, 10-12 week, weight 230 ± 10 g, $n=28$, respectively) were purchased from military science laboratory animal center of Chinese liberation army academy [SCXK (army), 2012-2004]. The rats were divided into 8 groups according to the random number table method (7 rats per group) and named: Wistar SHAM, SD SHAM, Wistar 2 hour (after myocardial infarction), SD 2h, Wistar 2 day (after myocardial infarction), SD 2d, Wistar 2 week (after myocardial infarction) and SD 2w. All animals were sacrificed after experimental procedure with potassium chloride. All experiments were conducted in accordance with the ethical requirements of Tianjin Medical University and the Third Central Hospital.

2.2 Acute Myocardial Infarction

The purchased animals were kept in the laboratory for 1 week (room temperature 25 ± 1 °C, each 12 hours of light and shade). Before operation, weighing and chloral hydrate (intraperitoneal, 0.3 ml / 100 g, 10%) as well as atropine (0.2 ml) were applied to anesthesia. Heart was manually exposed from the 4th intercostal space with endotracheal intubation through neck small incision aid (Fig. S1) and the left coronary artery was located, sutured and ligated at a site about 1 mm from its origin, which induced roughly 50% ischemia of the left ventricle. After ligation, observation of myocardial color changes can roughly estimate infarction area and confirm the effect of ligation at the same time. To ensure the survival rate, skilled model-making technician was needed to shorten the time of thoracotomy. Then the chest cavity of the rats was drained and when the reddish bloody fluid was extracted, stop the procedure.

Intraperitoneal antibiotics were injected to prevent postoperative infection and the rats were placed in clean cages, kept separately and warm. The SHAM groups were the same as operative groups without ligation.

2.3 ECG measurement

Biopac small animal physiological instrument ECG physiological measurement module was applied to do rat real-time ECG monitoring during operation. Infarction was considered successful following a ST elevation on ECG.

2.4 Cardiac functions measurement

CO and HR were measured by PowerLab physiological measurement instrument and LabChart physiological measurement system. Two-point calibration method was adopted to measure the results of the enrolled rats. The data processing system of LabChart software was used to record the temperature of low-temperature physiological saline, injection volume, injection time, and the differences in arteriovenous blood temperature and calculate to obtain the data of the rats.

To further analyze why the tendency of 2d groups was different from other two time points, echocardiography (isoflurane, 1.5% in air) was applied to measure the diastolic and systolic volume as well as left ventricle ejection fraction (LVEF) of these two rats' species as previously reported(9).

2.5 Animals Sample Collection

Wistar and SD rats were anesthetized at different time points, and a 10ml syringe was taken to puncture the inferior vena cava and draw blood from the inferior vena cava. The blood was drawn slowly, otherwise it was easy to cause hemolysis, which would have adverse effects on the later experiment. Then the samples were centrifuged to separate the plasma and preserved at -80°C until analysis.

2.6 Human Samples Collection

For the purposes of this prospective study, we enrolled 95 patients who were divided into four groups: the youth patient group (18–44 years old, AY group, n = 23) and elderly patient group (65–80 years old, AO group, n = 24) as well as two control groups (24 youth, SY group; 24 elderly, SO group) who were selected at the same time and within approximately the same age range after a physical examination. All patients were screened continuously from 405 patients treated from August 2013 to August 2014. The youth patients were required to provide a second blood draw during a follow-up visit 1 year after morbidity (FY group, n = 22, one lost). Because male patients comprised a dominant proportion of acute MI (AMI) morbidity in young adults (21/23, 91.3%), we selected a matched proportion of males in the healthy youth control group, healthy elderly control group, and AMI group.

The definition of ST-elevation MI (STEMI) was established according to the third universal definition of myocardial infarction symptoms(10). Patients with the following conditions were excluded: (1) secondary to non-atherosclerotic disease,(2) history of AMI, and (3) combination with cardiac shock, infection, liver or renal insufficiency, malignant tumor, or endocrine or metabolic diseases.

Three milliliters of venous blood were drawn from the peripheral vein immediately after successful primary percutaneous coronary intervention of emergency operation, defined as the recovered blood flow of the culprit vessel to TIMI3, and preserved in an ethylene diamine tetra acetic acid anticoagulant tube. The blood was then centrifuged to separate the plasma and preserved at -80°C until analysis. All samples were collected in accordance with the ethical guidelines and written consent protocols mandated by our hospital.

2.7 Samples pretreatment

Just before analysis, these rats' and humans' samples were thawed at room temperature, mixed with 100 μl plasma and 400 μl methanol, intensely vibrated for 30 s, and incubated at 4°C for 5 min to precipitate the protein; finally, the mixture was centrifuged at $15,000 \times g$ for 30 min at 4°C , then the supernatant was filtrated through a 0.22 μm membrane and analyzed. Equivalent volumes of some of the fluid from each sample were mixed for quality control (QC).

2.8 Sample analysis

Chemical reagents and instruments were showed in Supplementary Table 1. Chromatography conditions were as follows. Mobile phase: Phase A: 0.1% formic acid (volume ratio); Phase B: 95%ACN and 0.1% formic acid. Chromatographic separation was performed isocratically within 15 min, and the injection volume was 10 μl . The flow rate was set at 200 $\mu\text{l}/\text{min}$. The sample manager and column oven temperature were set at 4°C and 20°C , respectively. The chromatographic elution gradient was initialized at 5% Phase B and held for 3 min. Inconsecutive 10 min periods, Phase B was gradually escalated to 50%, and then a rapid increase in Phase B to 95% was completed within 3 min. After 4 min of maintaining the high volume of organic phase gradient, Phase B was immediately reduced to 5% and this elution gradient was used to balance the analytical column in the final 4 min.

MS was operating in the positive ion mode with an ion source voltage of 4.5 kV, a capillary voltage of 30 V, cone voltage of 150 V, desolvation temperature of 275°C , sheath gas flow of 30 arb, and assistant gas flow of 5 arb (99.999% nitrogen).

Data were collected over 15 min in centroid mode over the mass range 50–1000 m/z. The MS resolution was at 100,000 full-width half maximum, and the calibration standards were provided by Thermo Fisher Scientific (Caffeine, Ultramark 1621 and MRFA). MS/MS analysis was carried out with collision-induced dissociation collision energy 35 (normalization collision energy) and the collision gas was 99.999% helium.

There were 20, 23 and 22 QC samples throughout the test (equal volume mixture of each analyzed sample), respectively. Before the samples were tested, ten QC samples were analyzed continuously and there maining QC samples were inserted into the sequence after every ten samples were analyzed.

The sequence of samples was randomly generated by the Excel function before and after sample analysis (including QC), and cross-contamination was avoided by inserting a blank between adjacent samples. The whole experiment lasted 2100 min.

Metabolic pathways and functional analysis were applied using MetaboAnalyst4.0 (The Wishart Research Group, Canada). To further analyze the feasibility of these pathways, the similarities among three groups and subgroups had been conducted.

2.9 Statistical Analysis

GraphPad Prism version 7.0 and SPSS version 23.0 were used for statistical analysis. Results are shown as mean \pm s.e.m. Two-tailed student's t-testing and one- or two-way ANOVA with Bonferroni post-hoc analyses were used for comparisons between different groups. A P value less than 0.05 was considered significant. Sample sizes were designed with adequate power according to the literature and our previous studies. Randomization and blinding strategy were used whenever possible.

Results

3.1 Comparison of clinical parameters between Wistar and SD rats' groups

There were significant differences in indexes between Wistar and SD rats. Compared to SHAM groups, the MI groups showed higher HR and lower CO. Compared to Wistar rats' groups, SD rats' groups also showed higher HR and lower CO (Table 1).

In the 2 day after MI, there are increasing CO and decreasing HR both appearing in Wistar and SD rats. So, echocardiography was applied to measure the diastolic and systolic volume as well as LVEF. (Fig. S2, Tab. 1). There is no significant difference between the two rats' species, for instance, effective stroke volume, in 2 day after MI in SHAM and MI group, respectively (Fig. S2C).

3.2 Data pretreatment and quality control analysis

The total ion chromatograms were obtained from the UPLC/MS platform where differences in content between dozens of metabolites were identified (Fig. S3A-C). The data were imported into MZmine 2.0 software for pretreatment and standardization where 380 and 412 integral peaks were, respectively, detected in the ion chromatography extracted from QC and test samples.

The stability of the UPLC/MS system was assessed by analyzing the QC samples throughout the entire period. The principal component analysis (PCA) of around 22 data sets of QC samples was used to establish a PCA model with three principal components. The score plots of the QC sample sequence versus the first principal component [t(1)] were showed (Fig. S3D). In the test sample sequence, a QC sample was inserted after every ten test samples to evaluate the stability of the system during the entire analytical process; results showed that the detection system was indeed stable throughout the experiment after the first ten QC samples were injected (we set our QC standard according to a previously published article)(11). All the QC samples we inserted qualified, which allowed us to confirm that the analytical results were valid.

3.3 Different metabolic profiles among groups

The PCA models of Wistar rats, SD rats and human being ($R^2X=56\%$, $Q^2=29\%$; $R^2X=42.3\%$, $Q^2=15.2\%$; $R^2X = 30.3\%$, $Q^2 = 13.2\%$; respectively) were established. However, the clustering trends among groups were not obvious in the direction of the principal components, so we established an OPLS-DA model with seven, nine and twelve predictive principal components, respectively ($R^2X=75.8\%$, $R^2Y=69.6\%$, $Q^2=28.4\%$; $R^2X=47.6\%$, $R^2Y=20.5\%$, $Q^2=9.69\%$; $R^2X = 71.2\%$, $R^2Y = 79.6\%$, $Q^2 = 55.9\%$; respectively). There were significant distinguishing clustering trends between each group in the score plot of its principal component—in short, the OPLS-DA model made sufficient distinction between groups.

3.4 Screening and identification of characteristic metabolites

Again, metabolites with distinguishing characteristics were selected in the established OPLS-DA model (12). A total of identified metabolites were identified as listed in Table 2.

Two independent-sample nonparametric tests were used to compare differences in metabolic profiles between MI groups and SHAM/Normal group (Table 2). The levels of phospholipid (glycerophosphatide, sphingolipid) metabolites, as well as some free fatty acids and amino acids, were significantly up- or down-regulated. There are 42 significant plasma metabolites determined in our study, which consist of 19, 18 and 23 metabolites in Wistar, SD rats and human with acute MI, respectively.

Compared to the SHAM group, 19 and 23 metabolomics, such as Sphinganine, LysoPC(18:0) and etc., were screened in Wistar and SD MI groups (Tab. S2-S3). The blood samples of patients with AMI and normal had also been screened and there are 23 differential metabolomics (Tab. S4).

3.5 Metabolic pathways and functional analysis

MetaboAnalyst4.0 was applied to analyze the above most relevant metabolic pathways in greater detail (Fig. 1A-C). There are 6, 3 and 4 metabolic pathways to Wistar rats, SD rats and human, respectively (Metabolic pathway supplementary). Data about significant difference and impact of the pathway on those species were shown in Tab. 3.

Therefore, to discuss the similarity of Wistar and SD rats to human, metabolic pathway analysis was used to illustrate the most suitable species for human' metabolic research (Fig. 1D-H; Tab. S6). SD rats and human had two similar screened metabolic pathways, for instance, Sphingolipid metabolism and

Glycerophospholipid metabolism, whereas Wistar rats and human had all three screened metabolic pathways.

Some screened metabolomics between SD rats and human were controversial and the pathway of these metabolomics was analyzed through MetaboAnalyst 4.0 (Tab. S6), suggesting Sphingolipid metabolism has little impact on the researches of human's metabolic pathways.

3.6 Subgroup analysis in human's metabolomics

Subgroup analysis was applied in human's metabolomics. AO/SO, AY/SY, AY/AO and FY/SY were analyzed using MetaboAnalyst 4.0 (Tab. 2, Tab. S4). Further analysis of metabolic pathways demonstrated that Glycerophospholipid metabolism was only one which possessed metabolic pathway difference and did not affected by age and time, whereas Sphingolipid metabolism increased only in AMI when compared to SHAM group (Tab. S5).

Further research on homology between rats and human showed Sphingolipid metabolism in SD rats had little similarity to human's metabolic analysis, no matter to young or elders (Tab. S6). Besides, in FY group, Wistar and SD rats showed the same impact on Glycerophospholipid metabolism.

Discussion

Currently, AMI remains the leading "killer" in humans (1). Even after receiving timely reperfusion and the best possible drug therapy, there is still a large number of patients who fail to recover cardiac function after MI diagnosis – or even worse, whose cardiac health continue to decline after treatment (13). Early onset of myocardial infarction is most likely caused by a significant disruption in the body's metabolic system; thus, metabolomics can provide a direct molecular signature of cells that reflect changes in phenotypes and molecular physiology, and as such are very helpful for exploring pathogenesis and treatment efficacy (14-17). Sara E. et al. (17), for instance, identified a panel of biomarkers consisting of 19 identified metabolites in the serum of patients with STEMI. They provided a detailed map illustrating the most predominant altered metabolic pathways and the biochemical linkages among the biomarker metabolites identified in STEMI patients.

Metabolomics analysis may yield novel predictive biomarkers that will potentially allow for an earlier medical intervention. In addition, animal experiments, especially rats' experiment, about the relationship between MI and metabolic profiling are the cheapest and most convenient way to screen novel predictive biomarkers by metabolomics analysis. However, homology between rats and human has seen relatively little research.

The main rats' species, Wistar and SD rats, were applied to evaluate the similarity of metabolic profile to human being after MI. To ensure the welfare of animals, we also did endotracheal intubation through neck small incision aid to help decrease some complications (18) and increase the survival rate (19). The ECG, CO, HR and etc. were used to make sure the model-constructed success. After that, blood samples from Wistar, SD rats or human were collected to analyze the metabolomics among them, thus to choose the most suitable animal species to help explore human's metabolic potential target.

The characteristic ions obtained through simple statistical processing cannot be regarded as the final characteristic metabolites by default. The data comparison and processing of these metabolites are also required. At present, there are mainly two methods to determine the characteristics of ion metabolism based on literature and systematic description. Obviously, the most accurate and recognized method for the identification of ions is to use standard substances for comparison (12, 16). In this experiment, a large part of ions were compared with standard substances for ion, and then the results of experimental characteristic ions were obtained. However, the identification of ions in the experimental group that do not have the standard substance mainly relies on the following two ways of data identification: 1. The characteristic ions were scanned by MS/MS and compared through Secondary Mass Spectra and the theoretical fragments of HMDB identification results simulated by the built-in database of software Mass Frontier 6.0 (Thermo Fisher). The deviation between mass to charge ratio (m/z) of Secondary Mass Spectra and theoretical fragments is no more than 0.2. The theoretical debris can match the three-strong peak of secondary debris and cover more than 80% of the mass spectrum peak of characteristic ions, so, characteristic metabolites can be screened (20, 21); 2. The most commonly used method is to combine the plasmonuclear ratio of characteristic ions with the human metabolic database (<http://hmdb.ca/>; <http://www.metabolicatlas.org>) (22, 23) and Rat Genome Database (<http://rgd.mcg.edu>) (24) for m/z queries with ≤ 0.2 deviation. The retrieval results were verified in accordance with the exact charge number and the ionization method consistent with the experimental conditions, and the matching identification results were retained. Combined with the above three methods, our study of plasma metabolites in Wistar, SD rats and human with acute MI resulted in a total of 19, 18 and 23 standard characteristic metabolic ions, respectively.

These evidences presented thus far supports the idea that the first thing we should know is to investigate the difference of metabolic profile between Wistar and SD Rat after MI and compare the metabolomics with those of human being to help select the most suitable species to study some specific targets after MI.

Combining high performance liquid chromatography (HPLC) and mass spectrum technology platform with the HMDB and KEGG databases, we found three crucial metabolic pathways in animals and human metabolism research, Sphingolipid metabolism, glycerophospholipid metabolism and Glycerolipid metabolism. Corresponding products that are very important in these two metabolic pathways are found together: Sphinganine, Cer(d18:0/12:0), Phytosphingosine, LPA(0:0/16:0), LyoPc(18:1(9z)) and etc. The patients with AMI were determined and we found glycerophospholipid was significantly lower and most of sphingolipid is raised. It has been reported that both of them showed a downward trend on the 5th day (16, 25, 26). Sphinganine were also reported as a synthetic ceramide (27) or regulated by neutral sphingomyelinase. in previous literature (28), which explains the results of Wistar and SD rats' different changes. In addition, experimental studies have also suggested that Sphinganine plays a key role of signal transduction in AMI (29-31), thereby causing calcium overload of myocardial cells, reducing myocardial contractility and increasing apoptosis of myocardial cells. In summary, we can find Sphingosine and Ceramide are two related substances, and AMI is closely related to the metabolism of phospholipids, which can cause cell death. Glycerophospholipids and Glycerolipid metabolisms are important components of cell membranes, which can mediate the exchange of key ions in cell membranes, maintain the balance of substances in vivo, and mediate signal transduction. More attention should be paid to the fact that the

metabolites, LPA(0:0/16:0), LysoPC(20:1(11Z)) and LyoPc(18:1(9z)), are reduced sharply in both animal experiments(32) and human samples, which is likely to lead to abnormal metabolism of phospholipids and associated with a variety of cardiovascular diseases(33-35), thus affecting calcium ion influx and calcium ion overload(36, 37).

Of course, there are also some limitations. The repairment and angiogenesis after MI are regulated by some signal pathways spatio-temporally, such as WNT canonical signaling (38). But we only selected three time points of animals and one point of human, which may not explain the issues clearly just draw qualitative conclusions. Furthermore, due to surroundings and epigenetic, there may be some small differences within a strain. So, further researches are needed to illustrate this issue clearly.

Conclusions

Overall, according the metabolic pathway analysis of those similar metabolites among three groups, Sphingolipid metabolism in SD rats is not suggested to be substitute for human metabolic research and the effect of Wistar rats on metabonomic is better than that of SD rats because their metabolic pathways are relatively closer to human's real world, which can give us enlightenment and evidence for further researches on metabolic reactions. The results on homology of metabonomic between rats and human can also help investigate more specific targets, therefore, may be translated to clinic more easily.

Abbreviations

Abbreviation	Full Name
AMI	Acute myocardial infarction
GC-MC	Gas chromatography-mass spectrometry
LVEF	Left ventricular ejection fraction
LC-MS	Liquid chromatography-mass spectrometry
S/N	Signal/noise
ECG	Electrocardiogram
UPLC-MS	Ultra-performance liquid chromatography-mass spectrometry
MACE	Major adverse cardiovascular event
OPLS-DA	Orthogonal partial least square discrimination analysis
PCI	Percutaneous coronary intervention
TIC	Total ion chromatography
STEMI	ST-segment elevated myocardial infarction
PCA	Principle component analysis
ROC	Receiver operating characteristic curve
HMDB	human metabolome database
CID	collision induced dissociation
RT	Retention time
FMHW	full width half maximum
VIP	variable importance in projection
EF	Ejection Fraction
LVPW	Left ventricular posterior wall thickness
IVS	Interventricular septal thickness
Mean Vel	Mean aortic velocity
Peak Vel	Aortic peak velocity
LVMass	Left ventricular myocardial mass
LVVol(d)	Diastolic left ventricular volume
LVVol(s)	Systolic left ventricular volume
HR	Heart rate
Peak Vel	Peak Velocity
MeanGrad	Mean aortic pressure difference
Mean Vel	Mean aortic velocity
IP	Ischemic postconditioning
IR	Ischemia reperfusion
PCI	Percutaneous coronary intervention
KEGG	Kyoto Encyclopedia of Genes and Genomes
CO	Cardiac output
CABG	Coronary artery bypass graft

Declarations

Competing interests

On behalf of all authors, the corresponding author states that there is no conflict of interest. We do not want to upload raw data of metabolomics.

Funding

This work was financially supported by Tianjin science & technology commission (16YFZCSY01060, 17JCQNJC10000); Tianjin municipal commission of health and family planning (2014KR01) and Tianjin health industry (14KG112).

Author contributions

YZ analyzed the data about metabolomics, investigated the metabolic pathways, and was a major contributor in writing the manuscript. QZ, WX and ZD constructed the model and collected the rats' blood samples. LH collected the human samples. LZ and TL did the metabolomic analysis. All authors read and approved the final manuscript.

Declarations

Ethics, consent and permissions as well as Consent to publish

All experiments, included samples collection and analysis of animals and human, were conducted in accordance with the ethical requirements of Tianjin Medical University and the Third Central Hospital. All human participants had given the informed consent and we had obtained consent to publish from the participants to report individual patient data.

Acknowledgement

Not applicable.

References

1. Naghavi M, Abajobir AA, Abbafati C, Abbas KM, Abd-Allah F, Abera SF, et al. Global, regional, and national age-sex specific mortality for 264 causes of death, 1980–2016: a systematic analysis for the Global Burden of Disease Study 2016. *The Lancet*. 2017;390(10100):1151-210.
2. Sun L, Hao Y, Nie X, Zhang X, Yang G, Wang Q. Construction of PR39 recombinant AAV under control of the HRE promoter and the effect of recombinant AAV on gene therapy of ischemic heart disease. *Exp Ther Med*. 2012;4(5):811-4.
3. Parikh NI, Gona P, Larson MG, Fox CS, Benjamin EJ, Murabito JM, et al. Long-term trends in myocardial infarction incidence and case fatality in the National Heart, Lung, and Blood Institute's Framingham Heart study. *Circulation*. 2009;119(9):1203-10.
4. Gajarsa JJ, Kloner RA. Left ventricular remodeling in the post-infarction heart: a review of cellular, molecular mechanisms, and therapeutic modalities. (1573-7322 (Electronic)).
5. Panchal SK, Brown L. Rodent models for metabolic syndrome research. *J Biomed Biotechnol*. 2011;2011:351982.
6. Buettner R, Scholmerich J, Fahrenholtz C, Bollheimer LC, Bollheimer LC. High-fat diets: modeling the metabolic disorders of human obesity in rodents. (1930-7381 (Print)).
7. Briaud I, Kelpe CI, Fahrenholtz C, Johnson LM, Johnson LM, Fahrenholtz C, Tran POT, Tran Po Fau - Poitout V, Poitout V. Differential effects of hyperlipidemia on insulin secretion in islets of langerhans from hyperglycemic versus normoglycemic rats. (0012-1797 (Print)).
8. Davidson EP, Coppey LJ, Dake B, Yorek MA. Effect of Treatment of Sprague Dawley Rats with AVE7688, Enalapril, or Candoxatril on Diet-Induced Obesity. *J Obes*. 2011;2011.
9. GALRINHO RD, CIOBANU AO, RIMBAS RC, MANOLE CG, MARINESCU D, VINERANU D. New Echocardiographic Protocol for the Assessment of Experimental Myocardial Infarction in Rats. *A Journal of Clinical Medicine*. 2015;10(2):85-90.
10. Hani Jneid, Mahboob Alam, Salim S. Virani, Bozkurt B. Redefining Myocardial Infarction: What Is New In The ESC/ACCF/AHA/WHF Third Universal Definition Of Myocardial Infarction? *Methodist Debakey Cardiovasc J*. 2013; 9(3):169-72.
11. Chekmeneva E, Dos Santos Correia G, Gomez-Romero M, Stamler J, Chan Q, Elliott P, et al. Ultra-Performance Liquid Chromatography-High-Resolution Mass Spectrometry and Direct Infusion-High-Resolution Mass Spectrometry for Combined Exploratory and Targeted Metabolic Profiling of Human Urine. *J Proteome Res*. 2018;17(10):3492-502.
12. Zhang L, Huang Y, Lian M, Fan Z, Tian Y, Wang Y, et al. Metabolic profiling of hepatitis B virus-related hepatocellular carcinoma with diverse differentiation grades. *Oncol Lett*. 2017;13(3):1204-10.
13. Bian ZY, Wei X, Deng S, Tang QZ, Feng J, Zhang Y, et al. Disruption of mindin exacerbates cardiac hypertrophy and fibrosis. *J Mol Med (Berl)*. 2012;90(8):895-910.
14. Senn T, Hazen SL, Tang WH. Translating metabolomics to cardiovascular biomarkers. *Prog Cardiovasc Dis*. 2012;55(1):70-6.
15. Kohlhauser M, Dawkins S, Costa ASH, Lee R, Young T, Pell VR, et al. Metabolomic Profiling in Acute ST-Segment-Elevation Myocardial Infarction Identifies Succinate as an Early Marker of Human Ischemia-Reperfusion Injury. *J Am Heart Assoc*. 2018;7(8).
16. Huang L, Li T, Liu YW, Zhang L, Dong ZH, Liu SY, et al. Plasma Metabolic Profile Determination in Young ST-segment Elevation Myocardial Infarction Patients with Ischemia and Reperfusion: Ultra-performance Liquid Chromatography and Mass Spectrometry for Pathway Analysis. *Chin Med J (Engl)*. 2016;129(9):1078-86.
17. Ali SE, Farag MA, Holvoet P, Hanafi RS, Gad MZ. A Comparative Metabolomics Approach Reveals Early Biomarkers for Metabolic Response to Acute Myocardial Infarction. *Sci Rep*. 2016;6:36359.
18. Casey JD, Janz DR, Russell DW, Vonderhaar DJ, Joffe AM, Dischert KM, et al. Manual ventilation to prevent hypoxaemia during endotracheal intubation of critically ill adults: protocol and statistical analysis plan for a multicentre randomised trial. *BMJ Open*. 2018;8(8):e022139.

19. Hiltunen P, Jantti H, Silfvast T, Kuisma M, Kurola J, group FPs. Airway management in out-of-hospital cardiac arrest in Finland: current practices and outcomes. *Scand J Trauma Resusc Emerg Med.* 2016;24:49.
20. Shahidi-Latham S, Pribil P. Identification and Distribution of a Reserpine Metabolite in Dosed Whole-body Rat Tissue using MS and MS/MS Mass Spectrometric Imaging. *Journal of Biomolecular Techniques : JBT.* 2010;21(3 Suppl):S39-S.
21. Stanley BA, Gundry RL, Cotte RJ, Eyk JEV. Heart disease, clinical proteomics and mass spectrometry. *Dis Markers.* 2004;20(3):167-78.
22. Pornputtpong N, Nookaew I, Nielsen J. Human metabolic atlas: an online resource for human metabolism. *Database (Oxford).* 2015;2015:bav068.
23. Wishart DS, Knox C, Guo AC, Eisner R, Young N, Gautam B, et al. HMDB: a knowledgebase for the human metabolome. *Nucleic Acids Res.* 2009;37(Database issue):D603-10.
24. Wang SJ, Lauderkind SJ, Hayman GT, Smith JR, Petri V, Lowry TF, et al. Analysis of disease-associated objects at the Rat Genome Database. *Database (Oxford).* 2013;2013:bat046.
25. Hicks AA, Pramstaller PP, Johansson A, Vitart V, Rudan I, Ugoicsai P, et al. Genetic determinants of circulating sphingolipid concentrations in European populations. *PLoS Genet.* 2009;5(10):e1000672.
26. Sansbury BE, DeMartino AM, Xie Z, Brooks AC, Brainard RE, Watson LJ, et al. Metabolomic analysis of pressure-overloaded and infarcted mouse hearts. *Circ Heart Fail.* 2014;7(4):634-42.
27. Haynie KR, Vandanmagsar B, Wicks SE, Zhang J, Mynatt RL. Inhibition of carnitine palmytoyltransferase1b induces cardiac hypertrophy and mortality in mice. *Diabetes Obes Metab.* 2014;16(8):757-60.
28. Pavoine C, Pecker F. Sphingomyelinases: their regulation and roles in cardiovascular pathophysiology. *Cardiovascular research.* 2009;82(2):175-83.
29. Karliner JS. Sphingosine kinase and sphingosine 1-phosphate in the heart: a decade of progress. *Biochim Biophys Acta.* 2013;1831(1):203-12.
30. Egom EEA, Mohamed TMA, Mamas MA, Shi Y, Liu W, Chirico D, et al. Activation of Pak1/Akt/eNOS signaling following sphingosine-1-phosphate release as part of a mechanism protecting cardiomyocytes against ischemic cell injury. *American journal of physiology Heart and circulatory physiology.* 2011;301(4):H1487-H95.
31. Milhas D, Clarke CJ, Hannun YA. Sphingomyelin metabolism at the plasma membrane: implications for bioactive sphingolipids. *FEBS Lett.* 2010;584(9):1887-94.
32. Chien KR, Peau RG, Farber JL. Ischemic Myocardial Cell Injury. Prevention by chlorpromazine of an accelerated phospholipid degradation and associated membrane dysfunction. *Am J Pathol.* 97(3):505-29.
33. Hardwick JP, Eckman K, Lee YK, Abdelmegeed MA, Esterle A, Chilian WM, et al. Eicosanoids in metabolic syndrome. *Adv Pharmacol.* 2013;66:157-266.
34. Khandoga AL, Pandey D, Welsch U, Brandl R, Siess W. GPR92/LPA(5) lysophosphatidate receptor mediates megakaryocytic cell shape change induced by human atherosclerotic plaques. *Cardiovasc Res.* 2011;90(1):157-64.
35. Schober A, Siess W. Lysophosphatidic acid in atherosclerotic diseases. *Br J Pharmacol.* 2012;167(3):465-82.
36. Ueda N. Ceramide-induced apoptosis in renal tubular cells: a role of mitochondria and sphingosine-1-phosphate. *Int J Mol Sci.* 2015;16(3):5076-124.
37. Czubowicz K, Strosznajder R. Ceramide in the molecular mechanisms of neuronal cell death. The role of sphingosine-1-phosphate. *Mol Neurobiol.* 2014;50(1):26-37.
38. Palevski D, Levin-Kotler LP, Kain D, Naftali-Shani N, Landa N, Ben-Mordechai T, et al. Loss of Macrophage Wnt Secretion Improves Remodeling and Function After Myocardial Infarction in Mice. *J Am Heart Assoc.* 2017;6(1).

Tables

Table 1. Clinical characteristic after MI.

Characteristics	Wistar MI	SD MI
N per group	7	7
Weight, g	237.2±5.3	233.7±7.4
CO		
2h	32.46±1.20	29.18±1.10
2d	32.95±0.97	29.36±1.30
2w	32.60±1.14	26.28±1.25
SHAM	55.02±1.02	43.36±1.78
HR		
2h	323.21±16.65	437.30±5.94
2d	300.20±13.79	422.87±11.49
2w	325.12±10.23	337.06±16.63
SHAM	280.21±15.26	404.26±6.60
LVEF		
2d	35.50±2.35	32.14±1.77
SHAM	62.15±2.31	59.33±2.79
LV Vol;d, uL		
2d	301.25±19.24	291.60±17.21
SHAM	332.16±2.14	322.04±1.32
LV Vol;s, uL		
2d	188.62±14.22	197.87±12.39
SHAM	106.13±7.26	127.97±5.33

Table 2. Metabolite identification results and the difference among three groups

m/z	RT(min)	Metabolite	Wistar rats			SD rats			Human				
			2h/S	2d/S	2w/s	2h/S	2d/S	2w/s	AMI/N	AO/SO	AY/SY	AY/AO	FY/SY
302.3	6.72781	Sphinganine	Up*	-	-	Down*	Down*	Down*	Up*	Up*	Up*	-	-
494.323	6.94713	LysoPC(16:1(9Z))	-	-	-	-	-	-	Down*	-	-	-	-
546.352	6.60857	LysoPC(18:0)	Down*	-	-	-	-	-	Down*	Down*	Down*	-	Down*
508.375	8.03549	LysoPC(P-18:0)	-	-	-	Down*	Down*	Down*	Down*	Down*	Down*	-	Down*
506.359	8.58556	LysoPC(P-18:1(9Z))	-	-	-	-	-	-	-	Down*	Down*	-	Down*
522.354	7.66455	LysoPC(18:1(9Z))	Down*	Down*	Down*	-	-	-	Down*	-	-	-	-
522.354	7.66455	LysoPC(18:1(11Z))	-	-	-	-	-	-	-	Down*	Down*	-	-
337.274	7.05147	LysoPC(18:2(9Z,12Z))	-	-	-	Down*	Down*	Down*	Down*	-	-	-	-
540.305	6.80829	LysoPC(18:3(6Z,9Z,12Z))	-	-	-	-	-	-	Down*	Down*	Down*	Up*	-
490.29	6.76246	LysoPC(14:0)	Up*	-	-	-	-	-	-	-	-	-	-
566.32	7.10287	LysoPC(20:4(8Z,11Z,14Z,17Z))	-	-	-	-	-	-	Up*	-	-	-	-
550.386	8.77023	LysoPC(20:1(11Z))	-	-	-	Down*	Down*	-	Down*	Down*	Down*	-	Down*
570.352	7.86944	LysoPC(20:2(11Z,14Z))	-	-	-	-	-	-	Down*	Down*	Down*	-	Down*
544.338	7.11841	LysoPC(20:4(5Z,8Z,11Z,14Z))	-	-	-	-	-	-	-	Down*	-	-	-
570.356	7.37359	LysoPC(22:5(7Z,10Z, 13Z,16Z,19Z))	Up*	-	-	-	-	-	-	-	-	-	-
590.32	7.07064	LysoPC(22:6(4Z,7Z,10Z,13Z,16Z,19Z))	-	-	-	-	-	-	Up*	-	-	-	-
496.34	7.52633	LysoPC(16:0)	Down*	-	-	Down*	Down*	Up*	-	-	-	-	-
502.33	7.0517	LysoPC(P-16:0)	-	-	-	Down*	Down*	Down*	Down*	-	-	-	-
433.232	7.36116	LPA(0:0/16:0)	Down*	Down*	Down*	-	-	-	Down*	-	-	-	-
510.354	7.95221	LysoPC(17:0)	-	-	-	-	-	-	Down*	Down*	Down*	Down*	-
461.263	8.17757	LPA(0:0/18:0)	Up*	Up*	Up*	-	-	-	-	-	-	-	-
487.286	8.57992	PA(20:4(5Z,8Z,11Z,14Z) e/2:0)	-	-	-	-	-	-	-	Down*	Down*	Up*	Down*
288.191	4.50854	Estrone	Up*	-	-	-	-	-	-	-	-	-	-
135.003	0.717129	3-Furoic acid	Up*	-	-	Up*	Up*	Up*	-	-	-	-	-
210.05	1.13129	Indoleacrylic acid	Up*	Up*	-	-	-	-	-	-	-	-	-
311.258	6.94738	(R)2-Hydroxysterculic acid	Up*	-	-	Up*	Up*	Up*	-	-	-	-	-
346.331	6.74818	2-hydroxyphytanic acid	-	-	-	-	-	-	-	-	Up*	-	-
250.079	0.73948	Deoxyadenosine	Up*	-	-	-	-	-	-	-	-	-	-
176.065	0.93844	Guanidinosuccinic acid	Up*	Up*	-	-	-	-	-	-	-	-	-
340.279	6.21121	Phytosphingosine	Down*	Down*	Down*	Down*	Down*	Down*	Down*	-	-	-	-
247.128	4.68701	Aspartyl-Isoleucine	Up*	Up*	Up*	-	-	-	-	-	-	-	-
201.123	4.50321	Epinephrine	Up*	Up*	-	-	-	-	-	-	-	-	-
214.01	0.711787	L-Aspartyl-4-phosphate	Up*	Up*	Up*	-	-	-	-	-	-	-	-
484.464	9.44252	Cer(d18:0/12:0)	Up*	-	-	-	-	-	Up*	Up*	Up*	Up*	Up*
556.529	10.4299	Cer(t18:0/16:0)	-	-	-	-	-	-	-	Up*	Up*	Up*	Up*
507.272	8.08572	(3b,9R)-5-Megastigmene-3,9-diol 9-[apiosyl-(1->6)-glucoside]	-	-	-	Down*	Down*	Down*	-	-	-	-	-
445.269	7.79311	DHAP(18:0e)	-	-	-	Down*	Down*	Down*	-	-	-	-	-
358.368	7.67963	Behenic acid	-	-	-	Up*	Up*	Up*	-	-	-	-	-
520.341	7.0511	Pregnanetriol	-	-	-	Down*	Down*	Down*	-	-	-	-	-
356.351	7.40061	Catelaicid acid	-	-	-	Up*	Up*	Up*	Up*	Up*	Up*	-	Up*
312.326	7.28137	Phytal	-	-	-	-	-	-	-	Up*	Up*	Down*	-
495.248	4.54762	Leukotriene D5	-	-	-	-	-	-	-	Up*	-	-	-
284.294	6.74211	Octadecanamide	-	-	-	Down*	Down*	Down*	Up*	Up*	Up*	-	-
118.065	1.75456	Guanidoacetic acid	-	-	-	-	-	-	-	-	Down*	-	-
270.144	5.74974	Threoninyl-lysine	-	-	-	-	-	-	-	-	Down*	-	Down*
569.309	4.50573	Protoporphyrinogen IX	-	-	-	-	-	-	Up*	-	-	-	-
328.321	6.76455	N,N-Dimethylsphingosine	-	-	-	-	-	-	Up*	-	-	-	-
402.393	7.8026	Cerebronic acid	-	-	-	-	-	-	Up*	-	-	-	-
256.263	6.20856	Palmitic amide	-	-	-	Up*	Up*	Up*	Up*	-	-	-	-
314.228	5.75407	9-Decenoylcarnitine	-	-	-	-	-	-	Down*	-	Down*	-	-
340.334	7.63485	Unknown	-	-	-	Up*	Up*	Up*	-	-	-	-	-
508.363	8.06805	Unknown	-	-	-	Down*	Down*	Down*	-	-	-	-	-

* P < 0.05; -: No significant difference.

m/z=row mass-to-charge ratio, RT= row retention time, LysoPC= lysophosphatidylcholine, Cer: Ceramide.

2h/S, 2d/S, 2w/S are the variation tendency of metabolite concentration of MI groups compared to SHAM group.

AMI/N is the variation tendency of metabolite concentration of patients with acute myocardial infarction compared normal human being.

AO: elders' AMI group, SO: elders' SHAM group, AY: young's' AMI group, SY: young's SHAM group, FY: young's follow-up 1year visit group.

Table 3. Metabolic pathway analysis.

	Wistar rats						SD rats						AM			
	Total	Expected	Hits	Raw p	$-\log(P)$	Impact	Total	Expected	Hits	Raw p	$-\log(p)$	Impact	Total	Expected	Hits	J
Sphingolipid metabolism	21	0.14979	2	0.0072241	4.9303	0.14286	21	0.13487	2	0.0020808	6.175	0.14286	25	0.041545	2	0.0
Glycerophospholipid metabolism	30	0.21398	2	0.01452	4.2322	0.24197	30	0.04	1	0.10265	2.2764	0.04444	39	0.064811	2	0.0
Glycerolipid metabolism	18	0.12839	1	0.11009	2.2065	0.0192							32	0.053178	1	0.
Tyrosine metabolism	42	0.29957	1	0.24007	1.4268	0.01279										
Purine metabolism	68	0.48502	1	0.36159	1.0172	0.00479										
Steroid hormone biosynthesis	70	0.49929	1	0.37018	0.99377	0.02803										
Biosynthesis of unsaturated fatty acids							42	0.06	1	0.14127	1.9571	<0.001				
Porphyrin and chlorophyll metabolism													104	0.042134	1	0

Figures

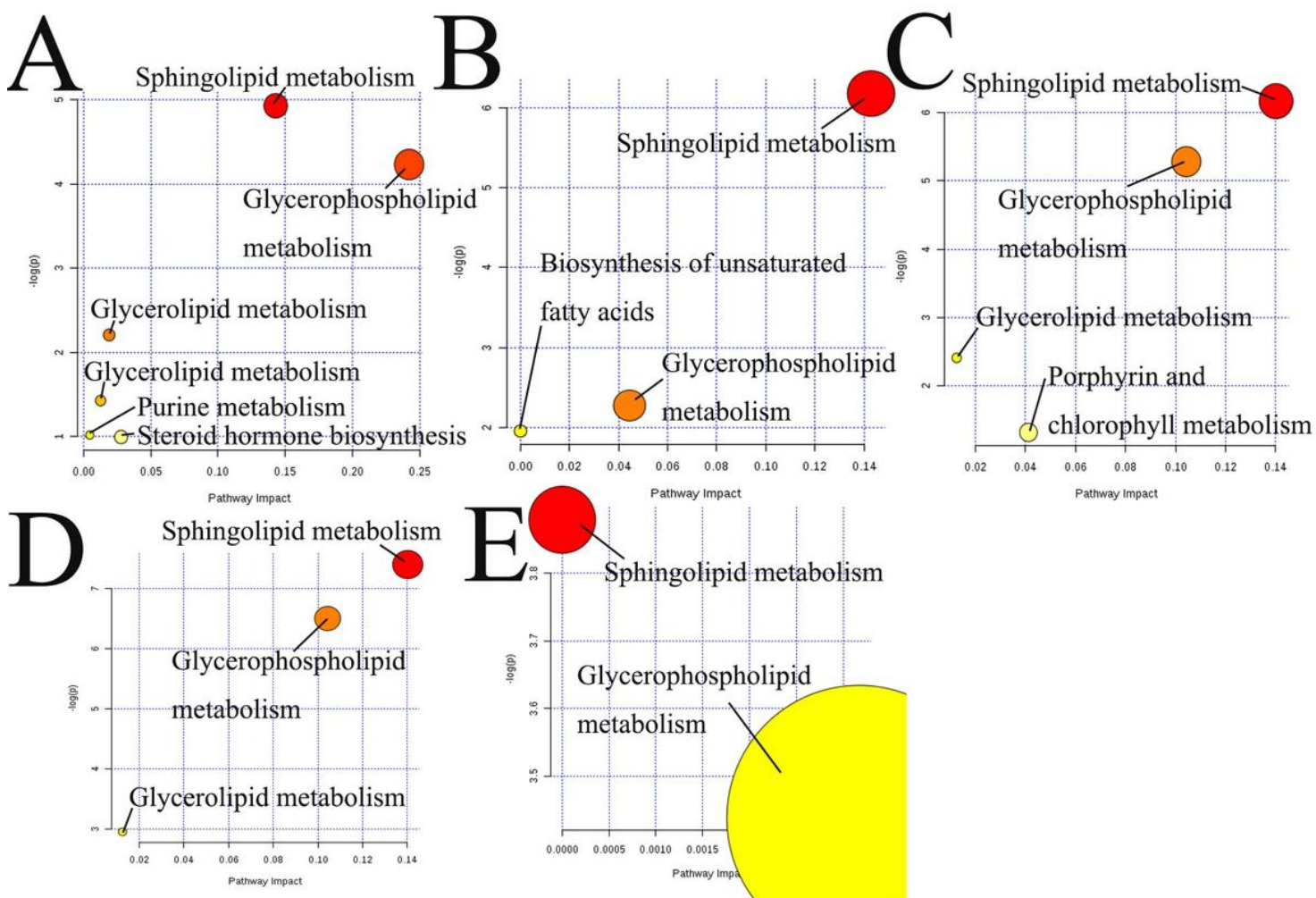


Figure 1

Signaling Pathway Analysis ABC. Pathways weight analysis of Wistar rats(A), SD rats(B) and human(C). D. Pathways weight analysis of the same metabolomics between Wistar rats and human being. E. Pathways weight analysis of the same metabolomics between SD rats and human being.

Supplementary Files

This is a list of supplementary files associated with this preprint. Click to download.

- [SupplementaryFigure3.tif](#)
- [SupplementaryFigure1.tif](#)
- [NC3RsARRIVEGuidelinesChecklistfillable.pdf](#)
- [SupplementaryFigure2.tif](#)
- [SupplementaryTable.docx](#)